Journal of Alloys and Compounds 620 (2015) 228–232

Contents lists available at ScienceDirect

Journal of Alloys and Compounds

journal homepage: www.elsevier.com/locate/jalcom

Hierarchical nanostructures assembled from ultrathin Bi_2WO_6 nanoflakes and their visible-light induced photocatalytic property

Xiong Wang [a,b,*], Peng Tian [a], Ying Lin [a], Li Li [a]

[a] School of Materials Science and Engineering, Nanjing University of Science and Technology, Nanjing 210094, China
[b] Department of Chemistry, Faculty of Science, National University of Singapore, 3 Science Drive 3, 117543, Singapore

ARTICLE INFO

Article history:
Received 18 June 2014
Received in revised form 15 September 2014
Accepted 16 September 2014
Available online 28 September 2014

Keywords:
Bismuth tungstate
Hydrothermal synthesis
Hierarchical nanostructures
Photocatalysis

ABSTRACT

With the aid of ethylene glycol and sodium dodecylbenzene sulfonate, the hierarchical Bi_2WO_6 nanoarchitectures assembled from nanoflakes could be attained by a facile solvothermal method. The synthetic strategy is versatile and environmentally friendly and a plausible growth-assembly process was proposed for the formation of the hierarchical nanostructures. The visible-light-irradiated photocatalytic activity was estimated by the degradation of rhodamine B. Compared with the sample prepared by a solid-state reaction, the visible-light-induced photocatalytic efficiency of the nanostructures was enhanced about 6 times. The photocatalysis tests show that the nanostructures exhibit excellent photocatalytic activity and recycling performance, which were mainly ascribed to the unique hierarchical nanostructures and are expected to offer promising applications in the field of wastewater treatment.

1. Introduction

With environmental and energy issues becoming even more prominent, exploiting renewable energy sources and developing efficient pollution control technologies have been attracting considerable attention [1–4]. Semiconductor photocatalyst materials have come into our sight to solve these problems since Honda discovered water splitting on TiO_2 electrodes in 1972 and Carey found organism degradation in TiO_2 solutions in 1976 [5,6]. Up to date, TiO_2 has been proven to be one of excellent semiconductor photocatalysts for hydrogen evolution and photodegradation. However, the major drawback of TiO_2 lies in the fact that it can only absorb a narrow band of solar spectrum in the UV-A region due to its large band gap (3.2 eV), which takes up only a tiny fraction of the total radiation reaching the earth's surface (~5%). To overcome the limitation and efficiently utilize the visible light, a variety of methods have been exploited to extend the responsive wavelength range of photocatalyst, including doping TiO_2 with other elements, and developing novel narrow-band-gap semiconductor catalysts [7–10]. Many research groups have reported some novel visible-light-induced photocatalysts, such as ZnO [11], WO_3 [12], CdS [13], $ZnIn_2S_4$–graphene nanocomposites [14], and Bi-based ternary oxides [15].

Among them, as one of the simplest oxides of the Aurivillius family, Bi_2WO_6 has a layered structure and is composed of perovskite-like $[WO_4]^{2-}$ layers sandwiched between bismuth oxide $[Bi_2O_2]^{2+}$ layers [16]. The formed internal electric fields between the slabs favor the efficient separation of photogenerated electron–hole pairs [17]. Furthermore, the hybridization of the O2p and Bi6s orbitals makes the valence band largely dispersed, resulting in a narrowed band gap and an expanded spectral absorption range. Thus such unique feature of Bi_2WO_6 can greatly enhance the photocatalytic performances.

Therefore, many methods have been introduced to synthesize Bi_2WO_6 powders, including refluxing process [18], electrospinning processes [19], low-temperature combustion synthesis [20], sol–gel [21], mechanochemical synthesis [22], and microwave-assisted method [23]. Hydrothermal method was also widely applied because of its convenience and controllability [24–27], but almost all of those mentioned above were carried out in the presence of nitric acid to get a homogenous solution due to the water insolubility of $Bi(NO_3)_3{\cdot}5H_2O$, or involving toxic, volatile, or expensive chemical substances. In this paper, ethylene glycol (EG) was introduced as solvent to form a homogeneous solution. Besides, sodium dodecylbenzene sulfonate (SDBS) was used as surfactant to achieve the hierarchical Bi_2WO_6 nanostructures. The visible-light-responsive photocatalytic activity was comparatively envalued by the degradation of rhodamine B (RhB) under visible light irradiation.

* Corresponding author at: Department of Chemistry, Faculty of Science, National University of Singapore, 3 Science Drive 3, 117543, Singapore. Tel./fax: +65 6516 4373.
E-mail address: xiongwang@njust.edu.cn (X. Wang).

http://dx.doi.org/10.1016/j.jallcom.2014.09.132
0925-8388/

This synthetic strategy is versatile and environmentally friendly and it will be applicable to the preparation of many other Bi-based functional inorganic materials.

2. Experimental

2.1. Synthesis

The Bi_2WO_6 powders were synthesized by a facile mixed-solvent hydrothermal method (denoted as H-BWO). All the reagents were used as received without further purification. In a typical synthesis, $Na_2WO_4{\cdot}2H_2O$ was added slowly into 60 ml EG solution containing stoichiometric amounts of $Bi(NO_3)_3{\cdot}5H_2O$ with the Bi/W molar ratio of 2 to form a transparent solution. SDBS (1.0 g) was also added and the mixture was stirred for 1 h at 50 °C. Ultimately, 20 mL distilled water was poured into the mixture. The resulting solution was transferred into a 100 mL Teflon-lined stainless autoclave and 80% of the autoclave volume was filled. The autoclave was subjected to hydrothermal treatment at 160 °C for 24 h under autogenous pressure and then air cooled to room temperature. The resulting precipitates were collected and washed with deionized water and absolute ethanol thoroughly and dried at 80 °C in air. For comparison, Bi_2WO_6 powders were also prepared by a conventional solid-state reaction based on a previous report [28]. Briefly, the high purity chemicals of Bi_2O_3 and WO_3 were mixed with 1:1 M ratio in an ethanol solution. The mixture was dried at 80 °C for 5 h and sintered at 900 °C for 12 h in air. The obtained sample was denoted as SSR-BWO.

2.2. Characterization

The crystal structure, phase purity, and lattice constants of the resulting samples were examined by X-ray diffraction (XRD) on a Bruker D8 Advance Diffractometer. The patterns were collected using unfiltered Cu Kα-radiation and the Bragg–Brentano geometry over the 2θ range 10–80°. The morphologies and microstructures of the as-prepared samples were analyzed by scanning electronic microscope (SEM) (Carl Zeiss EVO LS-15) and transmission electron microscope (TEM) (JEOL JEM-2100, accelerating voltage 200 kV). Nitrogen adsorption–desorption measurements were conducted at 77 K on a Micromeritics Tristar II 3020 M analyzer. The Brunauer–Emmett–Teller (BET) method was used to calculate the specific surface area. UV–Vis absorption spectra of the samples were obtained on a Shimadzu UV-2450 UV–Vis spectrophotometer.

The photocatalysis equipment is self-designed [29]. The visible-light source for catalytic reaction was a 500 W xenon lamp positioned in a quartz cold trap which was in the middle of multiposition cylindrical reaction vessel. The system was cooled by wind and water and maintained at room temperature. Appropriate cutoff filters were placed around the cold trap for complete removal of radiation below 400 nm to ensure that the catalysis of the RhB/Bi_2WO_6 system occurred only under visible light.

In every experiment, 20 mg Bi_2WO_6 was added to 40 ml RhB solution (10^{-5} mol/L) in a vessel. Before illumination, the suspensions were magnetically stirred in the dark for 1 h to ensure the establishment of an adsorption–desorption equilibrium between the photocatalyst and the dye molecules. Then the solution was exposed to visible light irradiation. The photocatalytic degradation rate of the products was calculated by the Beer's law based on the characteristic absorption peak at 553 nm for RhB using UV–Vis spectrophotometer (UV-2450, Shimadzu).

3. Results and discussion

3.1. Structure and morphology

The XRD pattern of the obtained powders is shown in Fig. 1. All diffraction peaks can be indexed to a pure orthorhombic Bi_2WO_6 (JCPDS card No.: 73-1126) and lattice parameters were estimated as a = 5.4630, b = 5.4474, c = 16.0890 Å. From the XRD pattern, no other characteristic diffraction peaks from impurities, such as bismuth oxides or WO_3, can be detected, indicating that the pure-phase Bi_2WO_6 could be obtained using the simple solvothermal method. The broadening of all the peaks means small crystal size of the resulting products. The average grain size of the sample was calculated from the XRD pattern according to the Scherrer formula ($D = k\lambda/\beta\cos\theta$, where D is the average grain size, k is the Scherrer constant related to the shape and index (hkl) of the crystals, λ is the wavelength of the X-ray, θ is the Blagg diffraction angle, and β is the full-width at half-maximum). The average crystallite size was estimated to be about 12 nm.

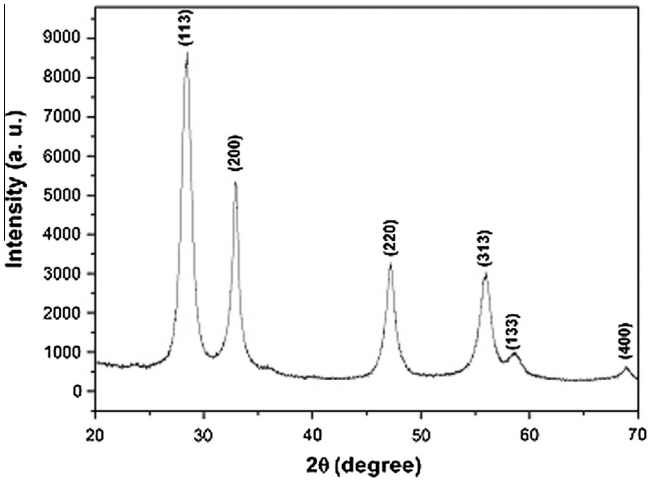

Fig. 1. XRD pattern of the obtained products.

The TEM and SEM images of the as-prepared Bi_2WO_6 are shown in Fig. 2. The morphology of the sample could be apparently identified as 3-dimensional (3D) hierarchical structures with nanoflakes as building blocks. From the HRTEM image of the edge of a nanoflake (Fig. 2b), the clear lattice fringes with interplanar spacing 0.324 nm can be observed, corresponding to the (1 1 3) plane of orthorhombic Bi_2WO_6. The single-crystal nature of the nanoflakes in the microstructures is revealed. Fig. 2(c) shows the electron diffraction (ED) pattern of the hierarchical structures. The general view of the sample (Fig. 2d), with the magnified inset, depicts that the morphology is uniform and the hierarchical structures assembled from nanoflakes are predominant with average diameter about 1 μm.

3.2. Formation process of the hierarchical structures

To examine the formation process of the hierarchical microstructures, the initial mixture hydrothermally treated for 2 h was subjected to further morphology observation. Fig. 3 exhibits the TEM images and the ED pattern of the sample. Fig. 3(a) affords a close-up view of the sample, and it can be seen that the sample consists of large amounts of nanoflakes with diameter ranging from 5 to 10 nm. Fig. 3(b) shows a magnified image of an individual nanoflake marked with a rectangle in Fig. 3(a), suggesting a loosened structure. Fig. 3(c) displays the HRTEM image with clear lattice fringes, corresponding to the (1 1 3) plane of orthorhombic Bi_2WO_6.

Thus, the formation of the hierarchical nanostructures can be concluded as a growth-assembly process. Bi_2WO_6 nuclei were formed at the early stage from Bi^{3+} and WO_4^{2-} in a supersaturated solution. Due to the high intrinsic anisotropic properties of orthorhombic Bi_2WO_6, these formed nuclei prefer to grow into flaky structure with single-crystal nature under the mild hydrothermal conditions. Then the nanoflakes self-assembled together to constitute 3D nanoarchitectures driven by the desire to further reduce Gibbs free energy with the aid of SDBS. With prolonging the reaction time, the well-developed hierarchical nanostructures were formed through the dissolution–recrystallization process. Ultimately, the hierarchical nanoarchitectures became predominant at the expense of the dispersed nanoflakes. The detailed formation mechanism of Bi_2WO_6 hierarchical nanostructures in the process needs further investigation.

3.3. Photodegradation

The morphology and the synthetic strategy of a photocatalyst play an important role in influencing the photocatalytic